

Quantitative spinal cord MRI in MOG-antibody disease, neuromyelitis optica and multiple sclerosis

Romina Mariano,¹ Silvia Messina,¹ Adriana Roca-Fernandez,¹ Maria I. Leite,¹ Yazhuo Kong^{2,3,4} and Jacqueline A. Palace¹

Spinal cord involvement is a hallmark feature of multiple sclerosis, neuromyelitis optica with AQP4 antibodies and MOG-antibody disease. In this cross-sectional study we use quantitative spinal cord MRI to better understand these conditions, differentiate them and associate with relevant clinical outcomes. Eighty participants (20 in each disease group and 20 matched healthy volunteers) underwent spinal cord MRI (cervical cord: 3D T₁, 3D T₂, diffusion tensor imaging and magnetization transfer ratio; thoracic cord: 3D T₂), together with disability, pain and fatigue scoring. All participants had documented spinal cord involvement and were at least 6 months post an acute event. MRI scans were analysed using publicly available software. Those with AQP4-antibody disease showed a significant reduction in cervical cord cross-sectional area ($P = 0.038$), thoracic cord cross-sectional area ($P = 0.043$), cervical cord grey matter ($P = 0.011$), magnetization transfer ratio ($P \leq 0.001$), fractional anisotropy ($P = 0.004$) and increased mean diffusivity ($P = 0.008$). Those with multiple sclerosis showed significantly increased mean diffusivity ($P = 0.001$) and reduced fractional anisotropy ($P = 0.013$), grey matter volume ($P = 0.002$) and magnetization transfer ratio ($P = 0.011$). In AQP4-antibody disease the damage was localized to areas of the cord involved in the acute attack. In multiple sclerosis this relationship with lesions was absent. MOG-antibody disease did not show significant differences to healthy volunteers in any modality. However, when considering only areas involved at the time of the acute attack, a reduction in grey matter volume was found ($P = 0.023$). This suggests a predominant central grey matter component to MOG-antibody myelitis, which we hypothesize could be partially responsible for the significant residual sphincter dysfunction. Those with relapsing MOG-antibody disease showed a reduction in cord cross-sectional area compared to those with monophasic disease, even when relapses occurred elsewhere ($P = 0.012$). This suggests that relapsing MOG-antibody disease is a more severe phenotype. We then applied a principle component analysis, followed by an orthogonal partial least squares analysis. MOG-antibody disease was discriminated from both AQP4-antibody disease and multiple sclerosis with moderate predictive values. Finally, we assessed the clinical relevance of these metrics using a multiple regression model. Cervical cord cross-sectional area associated with disability scores ($B = -0.07$, $P = 0.0440$, $R^2 = 0.20$) and cervical cord spinothalamic tract fractional anisotropy associated with pain scores ($B = -19.57$, $P = 0.016$, $R^2 = 0.55$). No spinal cord metric captured fatigue. This work contributes to our understanding of myelitis in these conditions and highlights the clinical relevance of quantitative spinal cord MRI.

- 1 Nuffield Department of Clinical Neurosciences, University of Oxford, Oxford, UK
- 2 CAS Key Laboratory of Behavioral Science, Institute of Psychology, Chinese Academy of Sciences, Beijing 100101, China
- 3 Department of Psychology, University of Chinese Academy of Sciences, Beijing 100049, China
- 4 Wellcome Centre for Integrative Neuroimaging, University of Oxford, Oxford, UK

Correspondence to: Jacqueline A. Palace
Level 3, West Wing, John Radcliffe Hospital, Headley Way, Oxford, OX3 9DU, UK
E-mail: jacqueline.palace@ndcn.ox.ac.uk

Received April 19, 2020. Revised July 2, 2020. Accepted August 11, 2020.

© The Author(s) (2020). Published by Oxford University Press on behalf of the Guarantors of Brain. All rights reserved.

For permissions, please email: journals.permissions@oup.com

Correspondence may also be addressed to: Yazhuo Kong
16 Lincui Road, Chaoyang District, Beijing 100101, China
E-mail: kongyz@psych.ac.cn

Keywords: neuromyelitis optica; multiple sclerosis; transverse myelitis; neuroinflammation; white matter lesion

Abbreviations: Ab = antibody; CSA = cross-sectional area; EDSS = Expanded Disability Status Scale; MTR = magnetization transfer ratio; NMOSD = neuromyelitis optica spectrum disorder

Introduction

The most well-described inflammatory demyelinating CNS disease is multiple sclerosis, a T-cell predominant immunological disorder of unknown aetiology (Olsson *et al.*, 2016). More recently, two further diseases caused by antibodies have been described. Aquaporin-4 antibodies (AQP4-Ab) target the AQP4 water channels situated on astrocyte foot processes and cause a primary astrocytopathy with secondary demyelination and the clinical phenotype of neuromyelitis optica spectrum disorders (NMOSD) (Lucchinetti *et al.*, 2014). Myelin oligodendrocyte glycoprotein antibodies (MOG-Ab) target myelin and are associated with a primary demyelinating disease with a wider clinical phenotype (Kitley *et al.*, 2014).

Although there is clinical overlap, the underlying pathogenesis for each is unique causing important phenotype differences. Most notable is that multiple sclerosis is associated with chronic disease activity and progressive disability outside of relapse whereas the two antibody diseases cause a relapsing course with more severe relapses and stability in between relapses (Tan *et al.*, 2016). The presence of AQP4-Ab is an independent predictor for relapses and so all patients require long-term immunosuppression therapy to prevent relapses (Weinshenker *et al.*, 2006; Jarius *et al.*, 2012). In MOG-Ab disease, relapses occur in 34–46% of patients (Jurynczyk *et al.*, 2017b; Cobo-Calvo *et al.*, 2018; Senanayake *et al.*, 2018). Differences between the monophasic and relapsing cohorts of this condition are not yet understood. Understanding what drives the differences between and within these disease groups would offer essential information to our understanding of these conditions and to therapeutic development and outcome prediction.

Spinal cord involvement is a hallmark feature of all three conditions and spinal cord lesions are important because they are a major driver of clinical symptoms and may cause substantial disability (Ciccarelli *et al.*, 2019). The classically described MRI findings are short, asymmetrical lesions in multiple sclerosis and longitudinally extensive central lesions (≥ 3 vertebral segments) in both NMOSD and MOG-Ab disease (Ciccarelli *et al.*, 2019) with involvement of the conus being noted particularly in those with MOG-Abs (Mariano *et al.*, 2019). However, short lesions are being reported more commonly in MOG-Ab disease (Dubey *et al.*, 2019; Mariano *et al.*, 2019) and both short and asymptomatic lesions have been reported in patients with AQP4-Ab disease (Flanagan *et al.*, 2015a, b). Although clinical MRI

has provided sound guidelines for an approach to these conditions, there are limitations (Filippi *et al.*, 2019). The use of quantitative and non-conventional imaging gives more insight into the pathogenic process than conventional imaging. Spinal cord MRI is notably more challenging and has been most applied predominantly in multiple sclerosis but recent developments in improved acquisition and analysis have made more widespread application possible (Stroman *et al.*, 2015a, b).

In multiple sclerosis, measurements of spinal cord cross-sectional area (CSA), diffusion metrics and magnetization transfer ratio (MTR) have shown clinical relevance in terms of disability, prognosis and progression (Moccia *et al.*, 2019). In particular, CSA has been shown to be a highly relevant outcome (Casserly *et al.*, 2018) and as having potential as a primary outcome in clinical trials for progressive multiple sclerosis (Cawley *et al.*, 2018; Prados and Barkhof, 2018). Furthermore, it has been shown that diffusion imaging in specific tracts within the cord demonstrate a strong relationship with the relevant clinical outcomes (Naismith *et al.*, 2013). Few studies have shown that these imaging techniques are also applicable in NMOSD (Benedetti *et al.*, 2006; Klawiter *et al.*, 2012; Pessôa *et al.*, 2012; Liu *et al.*, 2015; Matthews *et al.*, 2015; Chien *et al.*, 2019). Finally, one study has looked at atrophy measurements in MOG-Ab disease but none to our knowledge have explored the use of other quantitative measures (Chien *et al.*, 2019). No standardized comparative study has been conducted using these non-conventional methods in the spinal cord across the three diseases and including healthy volunteers.

In this study we used multimodal MRI to study spinal cord involvement in AQP4-Ab-positive NMOSD and MOG-Ab disease and compared it to multiple sclerosis and healthy volunteers. MRI sequences that have shown clinical relevance were selected and clinical data were collected using established measures. We aim to assess if these markers can be used to differentiate these conditions, provide a better understanding of the underlying condition outside of an acute episode, and if they are clinically relevant.

Materials and methods

Ethics

All participants signed informed, written consent specific to this study, which was approved the Research Ethics Committee of Cambridge South and was obtained according to the

Declaration of Helsinki. The reporting of this research was done in conjunction with the STROBE supporting guidelines.

Diagnosis

Testing for MOG-Abs and AQP4-Abs was performed in the autoimmune neurology laboratory at the University of Oxford using cell-based assays, as previously described (Wingerchuk *et al.*, 2014; Waters *et al.*, 2015). In particular, the MOG-Ab assay was to full-length MOG with an IgG1-specific secondary antibody, which increases specificity. All those positive for MOG-Ab were negative for AQP4-Ab and vice versa. The diagnosis of relapsing-remitting multiple sclerosis was made by a trained neurologist according to the 2010 McDonald criteria and confirmed by a second trained neurologist prior to approaching the patient to participate. None of the patients with multiple sclerosis had atypical features.

Subjects

Our clinic database was screened for adult patients either positive for AQP4-Ab or MOG-Ab and at least one possible episode of cord involvement. Adult multiple sclerosis patients, recruited as a disease control, were approached at consecutive clinic visits if they were confirmed to be relapsing-remitting and to have spinal cord involvement (either symptomatic or asymptomatic). Healthy volunteers were recruited by advertising, as per our ethics regulations. We age and sex-matched these participants as closely as possible to the disease groups. Recruitment ran from January 2018 to March 2019.

Patients in any disease cohort were excluded if they were unwilling to participate, had any contraindication to MRI scanning, including claustrophobia, or had been diagnosed with a confounding neurological comorbidity.

Sample size considerations included the rarity of the diseases being studied and selecting only those with spinal cord involvement. Spinal cord disease occurs in roughly 27% of those with MOG-Ab disease (Jurynczyk *et al.*, 2017b) and 40% of those with AQP4-Ab disease (Pandit *et al.*, 2015), which further limits availability but it was important for the objectives of our study that we included only those with documented cord involvement. We designed the study to have the power to detect group differences in metrics based on data from previous studies (Benedetti *et al.*, 2006; Klawiter *et al.*, 2012; Pessôa *et al.*, 2012; Liu *et al.*, 2015; Matthews *et al.*, 2015; Chien *et al.*, 2019) using G*power (Faul *et al.*, 2007) as well as recommendations for imaging studies based on evidence from multiple sclerosis (Altmann *et al.*, 2014; Reich *et al.*, 2015).

Severity and treatment of acute attacks

The severity at nadir for the antibody mediated conditions was the same: median (range) 6.0 (3–9) in MOG-Ab disease and 6.0 (3–8) in AQP4-Ab disease.

In the antibody-mediated conditions, treatment of the acute attack is particularly important (Kleiter *et al.*, 2016). In the AQP4-Ab cohort, all patients were treated acutely in a range of 1–10 days from the onset of symptoms. A total of 45 myelitis attacks occurred in this cohort. Five (from three patients) were treated with intravenous methylprednisolone, followed by

plasma exchange; one was treated with high dose oral prednisolone and the remaining were all treated with intravenous methylprednisolone. In all cases the acute treatment was followed by a tapering dose of oral prednisolone and all of these patients were put on long-term immunosuppression thereafter. In the MOG-Ab cohort, all patients were treated acutely in a range of 1–9 days from the symptom onset. A total of 31 myelitis attacks occurred in this cohort. Twenty-five were treated with intravenous methylprednisolone. Five were treated with high dose oral prednisolone and one was untreated and resolved spontaneously. All those in the MOG-Ab cohort then received tapering oral prednisolone which continued for a range of 6 months to 1 year after their attack. Six of the relapsing MOG-Ab patients were started on an additional long-term immunosuppressant.

Cervical cord

The clinical scans were reviewed and compared to the research scans collected for this study and patients were categorized as follows: (i) lesion present in cervical cord on clinical scan and on follow-up research scan (persistent); (ii) lesion present on clinical scan but no longer identifiable on follow-up research scan (resolved); or (iii) no lesion in the cervical cord (no cervical).

Thoracic cord

In the thoracic cord, patients were categorized as either having had thoracic involvement (thoracic involvement) or not (no thoracic). The thoracic images were not further categorized into persistent or not as the axial imaging sequences were not applied in this region.

Study visit

This research study visit was conducted at least 6 months outside of an acute event in any disease cohort.

During the study visit we collected demographic characteristics (i.e. age at onset of the disease, sex, and self-reported race/ethnicity), date of onset of the disease (disease duration was then calculated from the onset to the date of the research study visit), current treatment, and relapse history, in particular the specific location of any episode of spinal cord involvement.

During the same visit, participants completed a Brief Pain Inventory and a Modified Fatigue Impact Scale (MFIS). An Expanded Disability Status Scale (EDSS) was conducted and each patient underwent a 1-h multimodal spinal cord MRI, described in detail below. Healthy volunteers underwent the same MRI scan.

MRI data acquisition

MRI scans were acquired on a 3 T Siemens Prisma at the Oxford Centre for Functional MRI of the Brain (FMRI) with a 64-channel head and neck coil and additional spine array.

The protocol included cervical cord 3D T₁ MPRAGE (repetition time: 2.3 s; echo time: 3.57 ms; flip angle 9°; phase encoding: A ≫ P; res: 0.8 × 0.8 × 0.8 mm³), 3D T₂ SPACE (repetition time: 1.5 s; echo time: 95 ms; GRAPPA 2; phase encoding: H ≫ F; res: 0.9 × 0.9 × 0.9 mm³), 2D T₂* MEDIC (repetition time: 5.6 s; echo time: 71 ms; GRAPPA 2; phase encoding: R ≫ L; res: 0.4 × 0.4 × 3 mm³, six echoes), DTI AP/

PA (repetition time: 2.9 s; echo time: 79 s; flip angle 80°; phase encoding: AP and PA; res: $1.5 \times 1.5 \times 4 \text{ mm}^3$, $b = 1000$, 32 directions), MT on/off (repetition time: 600 ms; echo time: 8.6 ms; res: $0.4 \times 0.4 \times 4 \text{ mm}^3$) and thoracic cord 3D T₂ (repetition time: 1.5 s; echo time: 136 ms; GRAPPA 2; phase encoding: A \gg P; res: $0.8 \times 0.8 \times 0.8 \text{ mm}^3$).

A standard operation procedure was developed to ensure uniform acquisition in terms of participant positioning and sequence set-up. As far as possible, scans were done at the same time of day and all participants were encouraged to remain well hydrated in the 24 h preceding the scan. The same researcher was present at all scans to ensure uniformity (R.M.).

MRI data processing and analysis

Data were processed with tools from Spinal Cord Toolbox (SCT) v4.0 (De Leener *et al.*, 2017) and FMRIB Software Library (FSL) 6.0 (Jenkinson *et al.*, 2012). See Fig. 1 for illustration of quantitative analysis.

Structural imaging

Cervical cord atrophy and lesion measurements

Cervical cord images were analysed to obtain mean CSA, number of lesions and lesion volume. 3D T₁ images were automatically segmented to generate a cord mask using the DeepSeg (De Leener *et al.*, 2017) tool in SCT and manually adjusted, when necessary, using the FSL viewer FSLEyes (McCarthy, 2019) in slices presenting low contrast between cord and CSF. T₁ images were labelled per segment and straightened before being registered to the PAM-50-T₁ spinal cord template from

SCT using a multi-step registration method based on non-linear transformations. Quality of registration was visually inspected using the quality control mechanism provided by SCT (De Leener *et al.*, 2017). CSA was calculated per vertebral level and the mean CSA from C1–C7 was used for statistical analysis.

Binary lesion masks were manually generated using both axial MEDIC and sagittal T₂-weighted images, which were co-registered and then confirmed by a blinded rater. In cases of discrepancy, a third rater reviewed the image.

Thoracic cord atrophy measurements

Thoracic cord images were analysed to obtain the mean CSA. 3D T₂ images were segmented to generate a cord mask using DeepSeg (De Leener *et al.*, 2017) and manually adjusted, when necessary, using the FSL viewer FSLEyes (McCarthy, 2019) in slices presenting low contrast between cord and CSF. A multi-step registration method based on non-linear transformations was used to register each magnetic resonance scan to the PAM-50-T₁ spinal cord template (De Leener *et al.*, 2017). Quality of registration was visually inspected using the quality control mechanism provided by SCT (De Leener *et al.*, 2017). CSA was calculated per vertebral level to encompass the whole thoracic cord but excluding the conus, therefore the mean CSA for each participant was taken from T₁ to one level above the conus.

Cervical cord diffusion tensor imaging

Diffusion data were acquired in two phase encoding directions: AP and PA and merged. FSL tools topup (Andersson *et al.*, 2003; Smith *et al.*, 2004) and eddy (Andersson and Sotiropoulos, 2016) were used for distortion correction. Dtifit (Jenkinson *et al.*, 2012) was then used to generate fractional

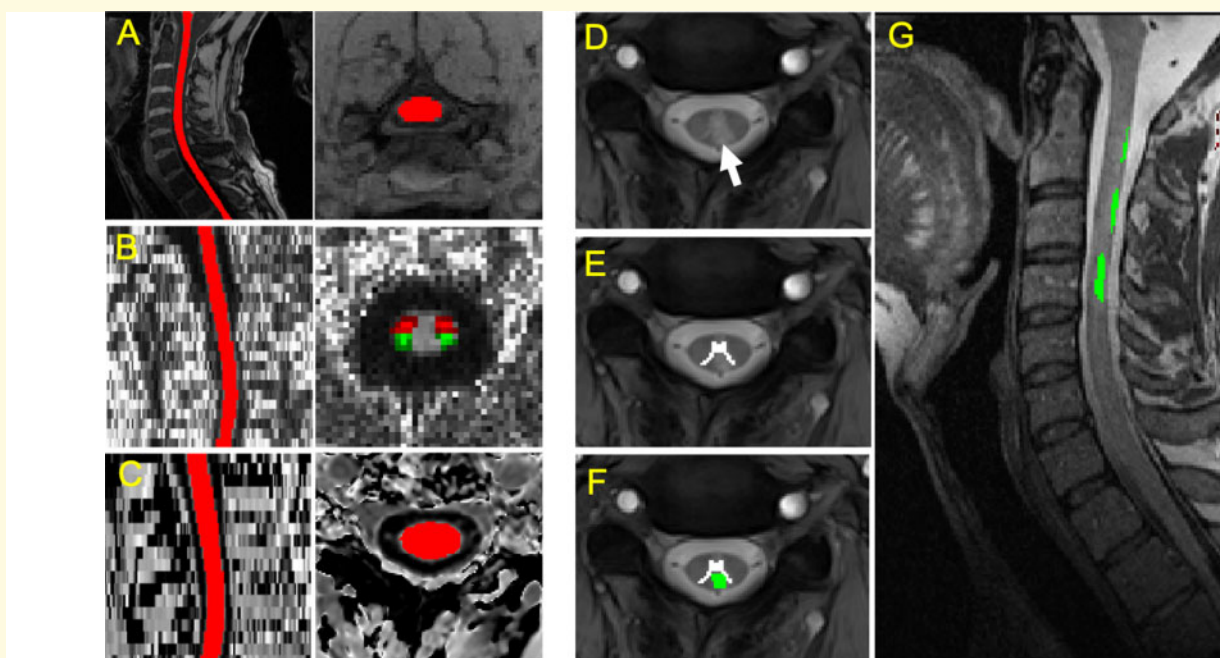


Figure 1 Imaging analysis. Examples of MRI metric analysis showing (A) cervical cord segmentation, (B) an fractional anisotropy map with cord segmentation and spinothalamic and corticospinal tract segmentation, (C) cervical cord MTR image with segmented cord, (D) T₂* axial image showing grey matter and a posterior lesion (white arrow) in multiple sclerosis, (E) with grey matter segmentation and (F) lesion mask, and then (G) co-registered with the sagittal image.

anisotropy and mean diffusivity maps. The cord was segmented within the native DTI space and this mask was applied to each quantitative map. A multi-step registration method based on non-linear transformations was used to register the fractional anisotropy/mean diffusivity image to the PAM-50 spinal cord template via the previously registered anatomical references with SCT tool `register_multimodal` (De Leener *et al.*, 2017). The template was then warped into fractional anisotropy/mean diffusivity image and metrics (whole cord, grey matter, white matter, lesional areas and normal-appearing cord) were then extracted per slice using `sct_extract_metric` (De Leener *et al.*, 2017). Tract-based analysis was done using the PAM-50 probability atlas, which includes the corticospinal and spinothalamic tracts.

Cervical cord magnetization transfer ratio

Magnetization transfer (MT)-on image was registered to MT-off image and MTR was computed using SCT. The MTR image was registered to the PAM-50 spinal cord template using the SCT tool `register_multimodal`, (De Leener *et al.*, 2017) as described above for the DTI analysis. The template was then warped into the map and metrics were extracted per slice using `sct_extract_metric` (De Leener *et al.*, 2017).

Statistical analysis

Statistical analysis was performed using SPSS v26.0 and GraphPad Prism version 6.0c. Mann-Whitney U-tests were used when comparing continuous variables. A chi-square test was used for comparing frequencies. Between-group comparisons were done using ANCOVA (general linear model in SPSS with age and sex as covariates) with *post hoc* Bonferroni. Within-group comparisons were done using ANOVA with *post hoc* Tukey or Kruskal-Wallis with *post hoc* Dunn test. Binomial logistic and multivariate regression models were used to identify factors associated with disability, pain and fatigue. *P*-values were two-tailed and statistical significance was set at 0.05. Principle component analysis was run using SIMCA v14.0.0.1359 (MKS Data Analytics Solutions, Sweden) with all MRI metrics that showed differences between groups to assess for spontaneous, unsupervised clustering. Thereafter a predictive regression analysis was run and an orthogonal partial least square analysis (OPLS-DA) model with seven cross-validation rounds and 200 iterations, comparing the three conditions in pairs (MOG-Ab versus AQP4-Ab, MOG-Ab versus multiple sclerosis, and AQP4-Ab versus multiple sclerosis). Each model was assessed for total variation in X (R2X), the total variation in Y (R2Y) and the accuracy of the prediction (q2). An R2Y of 100% suggests the model can explain all variation between groups. A higher R2Y and q2 mean a better separation. A q2 of 0.4 is generally accepted as the threshold for significance (Waterman *et al.*, 2010).

Data availability

All data were collected and stored in accordance with GDPR guidelines. Its availability is dependent on specific collaboration and data sharing agreements made with the host organization. Analysis software and methods are publicly available.

Results

Demographics

The study consisted of 80 participants (20 in each of the four groups). Where possible, key baseline characteristics were matched; however, there are important differences between these diseases that made complete matching impossible and this was handled by adjusting for differences in the statistical analysis (see below). The demographics of each group are represented in Table 1. Patients with AQP4-Ab tended to be older and with a female and non-Caucasian predominance, in keeping with demographics described in the literature (Kitley *et al.*, 2012) and the MOG-Ab group had the shortest disease duration.

Spinal cord involvement throughout disease course

All patients in the three disease cohorts were selected if they had spinal cord involvement during the course of their disease. In keeping with the recognized differences in the antibody diseases versus multiple sclerosis, patients with MOG-Ab and AQP4-Ab myelitis all had symptomatic transverse myelitis, and those with multiple sclerosis myelitis included both symptomatic and asymptomatic transverse myelitis lesions. The distribution of sagittal areas of the cord involved (cervical, thoracic and/or conus) is shown in Fig. 2 and highlights more conus involvement and lack of isolated cervical cord involvement in MOG-Ab disease, and more isolated cervical involvement in multiple sclerosis. The axial location of the lesions was central in 16/20 (80%) of the patients with MOG-Ab disease and 17/20 (85%) of those with AQP4-Ab. In the multiple sclerosis group, more than one lesion was present in each person with a total of 48 lesions noted. Nineteen of 48 (40%) were posterior and 29/48 (60%) were lateral; and none were central.

Clinical data

Motor

The median EDSS scores did not differ significantly between the three groups and are as follows: MOG-Ab 1.5 (0–8), AQP4-Ab 3.0 (0–8) and multiple sclerosis 2 (0–6). However, in patients with MOG-Ab, there was a single patient with an EDSS of 8, the remainder of the patients were all ≤ 3 (Table 1).

Sphincter

When considering long-term sphincter dysfunction, this occurred predominantly in those with MOG-Ab disease (13 with sphincter dysfunction, four requiring catheterization) when compared to AQP4-Ab (nine with sphincter dysfunction, two requiring catheterization) and multiple sclerosis (six with sphincter dysfunction, one requiring catheterization).

Table 1 Demographics and clinical features

	MOG	AQP4	Multiple sclerosis	Healthy volunteers	P-values
<i>n</i>	20	20	20	20	–
Mean age ± SD	43.4 ± 10.9	52.9 ± 12.5	45.3 ± 6.9	44.5 ± 14.3	0.010
Sex, female:male	10:10	13:7	11:9	12:8	0.796
Ethnicity (%)					0.001
Caucasian	20 (100)	11 (55)	20 (100)	18 (90)	
Afro-Caribbean	0 (0)	5 (25)	0 (0)	1 (5)	
Asian	0 (0)	4 (20)	0 (0)	1 (5)	
Phenotype (%)					< 0.001
Isolated TM	4 (20)	10 (50)	0 (0)	–	
TM + ON	10 (50)	4 (20)	0 (0)	–	
TM + BS/BR	5 (25)	4 (20)	8 (40)	–	
TM + BS/BR + ON	1 (5)	2 (10)	12 (60)	–	
Median disease duration in months (range)	40.1 (8.5–239.9)	141.5 (8.5–297.7)	147.1 (10.4–252.1)	–	0.015
Mean total number of attacks	2	3	3	–	0.949
Mean number of myelitis attacks	1.1	2.3	0.75 ^a	–	0.045
Median EDSS (range)	1.5 (0–8)	3 (0–8)	2 (0–6)	–	0.109
Sphincter dysfunction (number requiring catheter)	13 (4)	9 (2)	6 (1)	–	0.084
Mean BPI score ± SD	2.04 ± 4.16	5.66 ± 4.19	2.28 ± 3.45	0	0.009
Mean MFIS score ± SD	27.4 ± 18.92	35.26 ± 20.8	36.05 ± 14.27	8.9 ± 7.2	0.260

^aThis is the number of clinically symptomatic attacks.

BPI = Brief Pain Inventory; BR = brain; BS = brainstem; MFIS = Modified Fatigue Impact Scale; ON = optic neuritis; SD = standard deviation; TM = transverse myelitis.

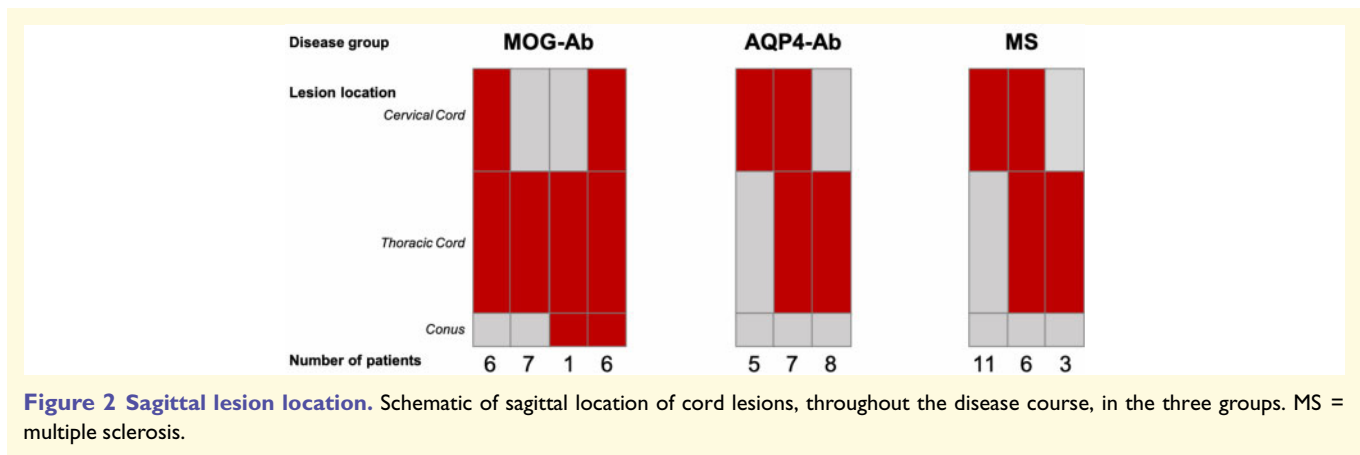


Figure 2 Sagittal lesion location. Schematic of sagittal location of cord lesions, throughout the disease course, in the three groups. MS = multiple sclerosis.

Pain

Those with AQP4-Abs had significantly higher scores than those with MOG-Ab ($P = 0.006$) and multiple sclerosis ($P = 0.045$) [$\chi^2(2) = 10.18$, $P = 0.006$].

Fatigue

Five patients with MOG-Abs, nine patients with AQP4-Abs, eight patients with multiple sclerosis and 0 healthy volunteers reached the diagnostic score of 38 on the MFIS. The mean MFIS scores in all three disease groups ($P = 0.006$, < 0.001 , < 0.001 , respectively) were significantly higher than healthy volunteers [$\chi^2(3) = 29.13$, $P \leq 0.001$].

Imaging results

Of the five imaging modalities for each of the 80 subjects, a total of 34 individual scans were not included because of

either poor quality or incomplete acquisition (six diffusion, 18 thoracic, four MTR, six grey matter segmentations). [Supplementary Table 1](#) shows all raw data means ± standard deviation (SD) as well as the estimated marginal means, after age and sex correction. The imaging results are shown graphically in [Fig. 3](#), the between-group comparison, and [Fig. 4](#), the within-group comparison based on whether there is a persistent lesion, a previous lesion that has now resolved on MRI or no lesion ever affecting that area. Key features of interest are highlighted below.

Cervical cord lesions

Nine of 12 AQP4-Abs and 14 of 17 multiple sclerosis cervical cord lesions were persistent, all 12 cervical cord lesions in MOG patients had resolved on structural imaging.

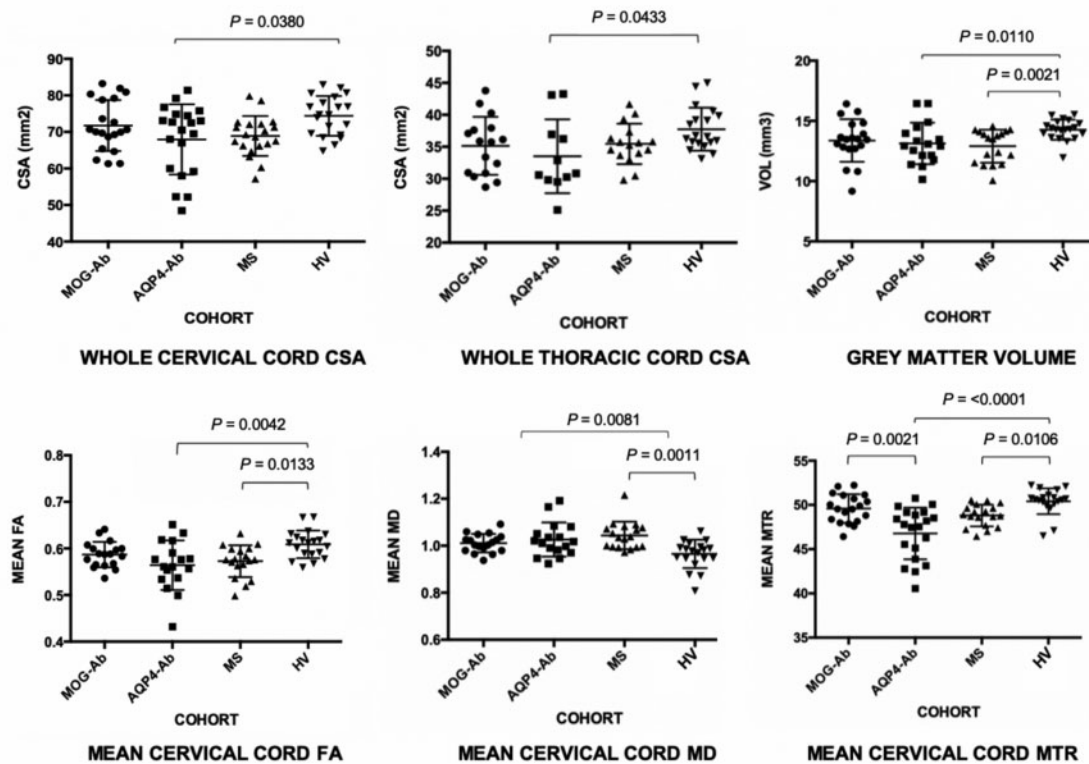


Figure 3 Between-group comparison. MRI metrics for each participant shown as raw data with lines for mean and standard deviation. *P*-values calculated with ANCOVA using age and sex as covariates and corrected for multiple comparisons using Bonferroni. FA = fractional anisotropy; HV = healthy volunteer; MD = mean diffusivity; MS = multiple sclerosis.

Mean cervical lesion volume did not differ between AQP4-Ab and multiple sclerosis (247.78 mm³ versus 305.56 mm³, *P* = 0.853); however, the mean number of lesions was significantly different with a greater number of lesions occurring in patients with multiple sclerosis (1 ± 0 versus 3 ± 2, *P* = 0.007), in keeping with the expected single, long lesions in AQP4-Ab disease.

Cervical cord cross-sectional area

The patients with AQP4-Abs showed a significant reduction in mean cervical cord CSA compared to the healthy volunteers (*P* = 0.038) [*F*(3,76) = 3.234, *P* = 0.027] with those with lesions driving this difference. This is evidenced by the significant difference between those with persistent lesions when compared to those without cervical cord involvement (*P* = 0.035) [*F*(2,17) = 3.788, *P* = 0.035]. The mean CSA of those without a history of cervical cord lesions being almost equivalent to healthy volunteers (73.86 mm² versus 74.38 mm², *P* = 0.815).

In those with multiple sclerosis there was a significant reduction compared to the healthy volunteers on direct comparison (68.96 mm² versus 74.71 mm², *P* = 0.005), not significant when comparing all groups. Additionally, the relationship with the lesion status was not significant (Fig. 4).

In those with MOG-Abs, there was no significant reduction in CSA overall compared to healthy volunteers or when comparing those with previous lesions in the cervical cord to those without (Fig. 4).

Thoracic cord cross-sectional area

Patients with AQP4-Abs just reached significance reduction in thoracic cord CSA compared to the healthy volunteers (*P* = 0.043) [*F*(3,46) = 3.252, *P* = 0.032]. This was driven by involvement of the thoracic cord with those that had never been affected by thoracic cord lesions having values comparable to the healthy volunteers group (37.11 mm² versus 37.91 mm², *P* = 0.677). This pattern is not evident in the multiple sclerosis group. There were no patients with MOG-Ab disease that did not have thoracic cord involvement and no thoracic lesions were persistent. The group mean did not differ statistically from the healthy volunteers; however, the only patient to reach EDSS > 6 in the MOG-Ab group had the smallest thoracic CSA (28.69 mm²).

Cervical cord grey matter volume

The patients with AQP4-Ab disease (*P* = 0.011) and with multiple sclerosis (*P* = 0.002) showed a significant

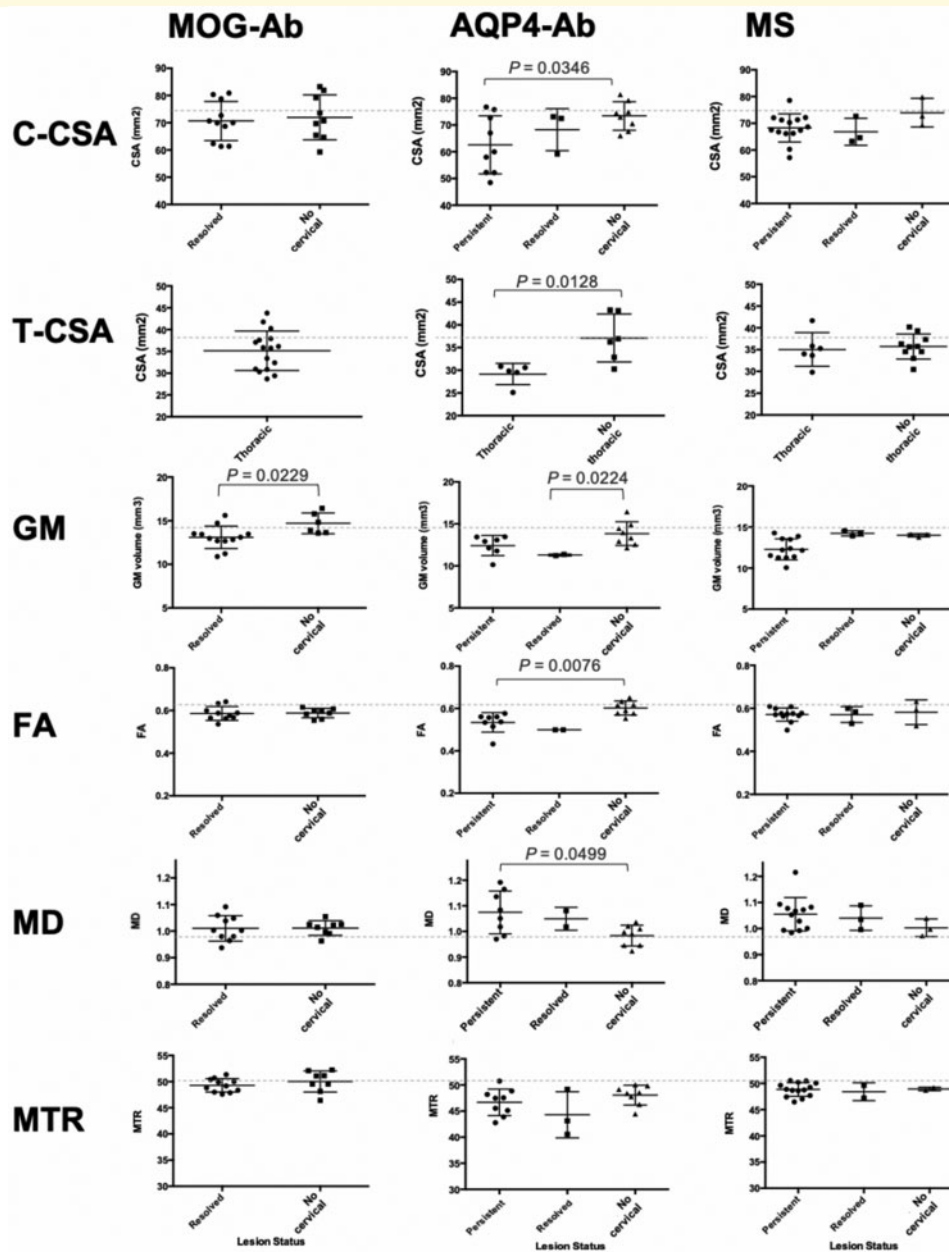


Figure 4 Within-group comparison. ANOVA (with *post hoc* Tukey) or Kruskal Wallis (with *post hoc* Dunn) results for within-group comparisons in each cohort, dividing patients by lesion status (x-axis) in the cervical cord (persistent, resolved or no cervical) and in the thoracic cord (thoracic or no thoracic). No patients with MOG-Ab had persistent cervical cord lesions. The dotted line represents the healthy volunteer (HV) mean for each modality. C-CSA = cervical cross-sectional area; FA = fractional anisotropy; GM = grey matter; MD = mean diffusivity; MS = multiple sclerosis; T-CSA = thoracic cross-sectional area.

reduction in mean cervical cord grey matter volume compared to the healthy volunteers [$F(3,74) = 3.984$, $P = 0.011$], but not in those with MOG-Ab. This effect was related to lesions in the AQP4 group (Fig. 4) and lower but not significantly so in persistent lesions in the multiple sclerosis group.

Patients with MOG-Ab and affected cervical cords had significantly reduced grey matter volume when compared to MOG-Ab without cervical cord lesions ($P = 0.023$) and

compared to the healthy volunteers ($P = 0.010$) [$\chi^2(1) = 11.01$, $P = 0.004$].

Cervical cord DTI

The mean fractional anisotropy in both those with AQP4-Ab ($P = 0.004$) and multiple sclerosis ($P = 0.013$) was significantly reduced compared to the healthy volunteers [$F(3,73) = 5.323$, $P = 0.002$]. This difference appeared to be

driven by the lesions in AQP4-Ab (Fig. 4). In MOG-Ab disease, the mean fractional anisotropy was comparable to healthy volunteers whether the cervical cord had been involved or not (Fig. 4).

Cervical lesional fractional anisotropy was significantly reduced compared to the normal-appearing spinal cord in both AQP4-Ab (0.46 ± 0.10 versus 0.56 ± 0.04 , $P = 0.037$) and multiple sclerosis (0.43 ± 0.06 versus 0.59 ± 0.02 , $P \leq 0.001$), and the mean lesional fractional anisotropy did not differ between groups (0.46 versus 0.43 , $P = 0.539$). MOG-Ab patients had fractional anisotropy values comparable to healthy control subjects whether previous lesions affected the cervical cord or not (Fig. 4).

The mean mean diffusivity was increased in those with AQP4-Ab ($P = 0.008$) and in multiple sclerosis ($P = 0.001$) compared to healthy volunteers [$F(3,73) = 6.794$, $P \leq 0.001$].

Cervical cord magnetization transfer ratio

Cervical cord MTR showed very similar patterns. Mean MTR was reduced in both AQP4-Ab ($P \leq 0.001$) and multiple sclerosis ($P = 0.011$) groups compared to healthy volunteers; as well as in AQP4-Ab when compared to the MOG-Ab group ($P = 0.002$) [$F(3,76) = 7.336$, $P \leq 0.001$]. Those with MOG-Ab showed no difference in mean MTR whether they had cervical cord involvement or not and, in both subsets, the mean MTR was comparable with healthy volunteers (49.28, 50.02 and 50.41, respectively).

Cervical lesional MTR was significantly reduced compared to the normal-appearing spinal cord in both AQP4-Ab (41.43 ± 2.08 versus 47.70 ± 4.85 , $P = 0.003$) and multiple sclerosis (43.10 ± 1.03 versus 49.40 ± 3.82 , $P \leq 0.001$) and the mean lesional values did not differ significantly between groups (41.43 ± 2.08 versus 43.10 ± 1.03 , $P = 0.269$). Supplementary Fig. 1 shows all lesional metrics compared to surrounding normal-appearing spinal cord in patients with persistent lesions.

Monophasic versus relapsing disease in MOG-Ab disease

These results are shown in Supplementary Fig. 2.

In those with MOG-Ab disease, volumetric measures of cervical cord area, thoracic cord area, as well as grey matter volume were lower in the 14 relapsing patients and lower values occurred in both those with relapsing myelitis ($n = 3$) as well as those whose relapses occurred elsewhere ($n = 11$). This reached significance in the thoracic cord, the location that was affected in all MOG-Ab patients, (33.60 ± 3.75 versus 40.75 ± 3.86 , $P = 0.002$) and held when comparing the monophasic to relapsing myelitis (40.75 ± 3.86 versus 29.48 ± 0.81 , $P = 0.003$) and those with non-myelitis relapses (40.75 ± 3.86 versus 34.96 ± 3.27 , $P = 0.012$). Additionally, when comparing thoracic cord volumes of those with relapsing MOG-Ab disease to healthy volunteers there was a significant difference (33.60 ± 3.75 versus 37.86 ± 3.22 , $P = 0.003$) but not when

comparing monophasic MOG-Ab disease to healthy volunteers (40.75 ± 3.86 versus 37.86 ± 3.22 , $P = 0.100$). Age and sex were included as covariates in all models.

Clinical association of cervical cord imaging metrics

We built a multiple regression model for each of the three clinical outcomes: EDSS, pain and fatigue (Supplementary Table 2). We included age, sex, disease duration and disease type and then included significantly associated MRI metrics using a stepwise regression model. Due to anatomical and physiological *a priori* hypotheses, we assessed associations between EDSS and corticospinal tract fractional anisotropy, and pain spinothalamic tract fractional anisotropy.

In the EDSS model, the mean cervical cord CSA was the only significant variable ($B = -0.07$, $P = 0.0440$, overall model $R^2 = 0.20$).

In the pain model, the fractional anisotropy in the spinothalamic tract ($B = -19.57$, $P = 0.016$), the presence of AQP4-Ab ($B = 14.08$, $P = 0.010$) and EDSS score ($B = 0.46$, $P = 0.002$) were significant predictors (overall model $R^2 = 0.55$). As no MRI metrics associated with fatigue, only clinical factors were included.

As disability and fatigue showed a significant relationship in the univariate analysis, we conducted a logistic regression using the cut-off of ≥ 38 to represent clinically significant fatigue. The odds ratio (OR) was 1.5 for every 1-point increase in EDSS [OR = 1.5, confidence interval (CI) = 1.05–2.15, $P = 0.038$].

Discriminatory analysis

To test the ability of these MRI measures to discriminate between diseases and predict the disease type, we used the MRI metrics in a principal component analysis. Variables included were as follows: mean cervical CSA, whole cervical cord MTR, whole cervical cord fractional anisotropy, whole cervical cord mean diffusivity, number of lesions, sagittal lesion location and length, cervical cord grey matter volume and thoracic cord volume. Patients with MOG-Ab tended to spontaneously separate (Fig. 5). We therefore applied discriminatory models to each pair separately using OPLS-DA. A moderately predictive model was created to distinguish MOG-Ab from multiple sclerosis ($q^2 = 0.43$, R2Y 68%) (Fig. 6A). The most important classifiers between MOG-Ab and multiple sclerosis were number of persistent lesions, sagittal lesion location (thoracic more predictive of MOG-Ab), whole cervical cord mean diffusivity and mean cervical cord CSA. A model was also built to distinguish MOG-Ab from AQP4-Ab ($q^2 = 0.51$, R2Y 59%) (Fig. 6B). The most important classifiers between MOG-Ab and AQP4-Ab were number of persistent lesions, sagittal lesion location (thoracic predictive of MOG-Ab) and whole cervical cord MTR. AQP4-Ab could not be distinguished significantly from multiple sclerosis ($q^2 = 0.37$, R2Y = 49%) (Fig. 6C).

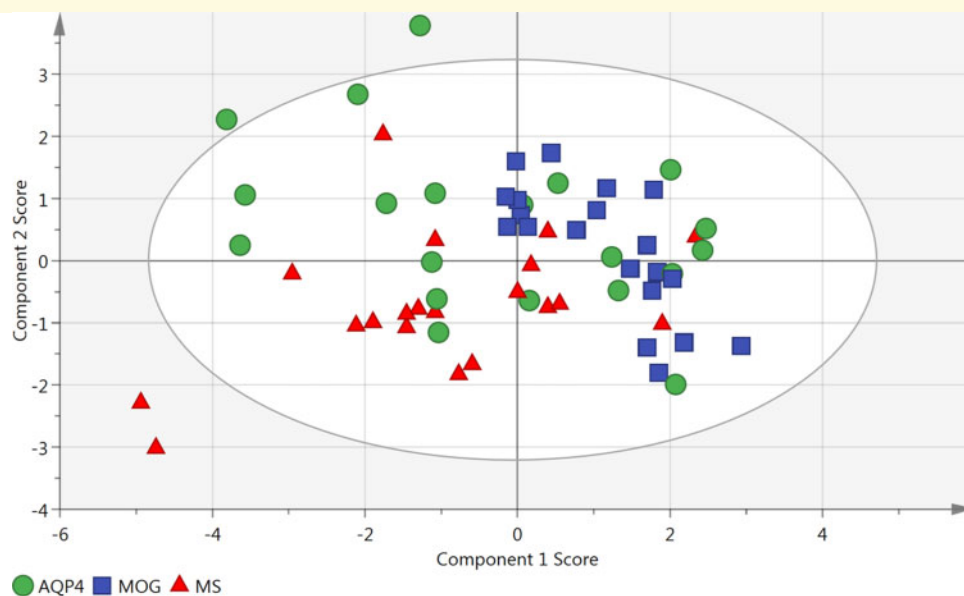


Figure 5 Principle component analysis. Principle component analysis showing the trend of clustering in the MOG-Ab group (blue square). MS = multiple sclerosis.

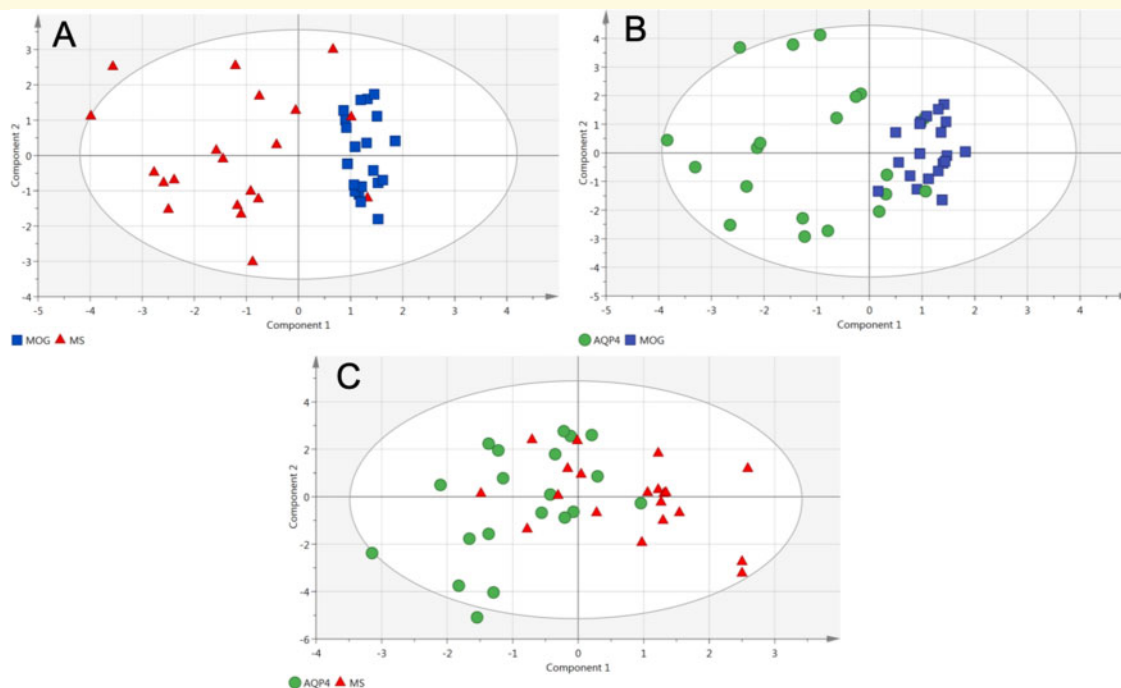


Figure 6 Discriminatory analysis. Orthogonal partial least squares analysis showing moderately predictive models for MOG-Ab and multiple sclerosis (MS) (A), MOG-Ab and AQP4-Ab (B), and AQP4-Ab and multiple sclerosis (C).

Discussion

This is the first paper, to our knowledge, that uses quantitative MRI methods to study spinal cord involvement in MOG-Ab disease and compare it with AQP4-Ab-positive NMOSD and multiple sclerosis. In particular, we highlight

that both patients with MOG-Ab and AQP4-Ab disease show changes only in the area of the cord affected by the lesion. In MOG-Ab there is evidence of atrophy in some cases, and this appears to more significantly involve the grey matter. However, it is milder than AQP4-Ab disease and in addition, in keeping with their good clinical recovery, those with

MOG-Ab show no difference to healthy volunteers in quantitative measures using diffusion and magnetization-weighted imaging after recovery from the myelitis. Additionally, these spinal cord MRI metrics show clinical relevance in terms of pain and disability, but not fatigue. Our results suggest that cervical cord CSA associates with EDSS and spinothalamic fractional anisotropy may be predictive of pain scores.

To understand the evolution of spinal cord involvement in these conditions it is important to consider findings throughout the disease course. Therefore, the results of our research MRI scans, conducted at least 6 months after an acute event, are presented in a way that is informed by the earlier presentations. None of the patients with MOG-Ab had persistent cord lesions. This is a clinically relevant finding as the imaging protocol is one used in clinical practice in many centres and may be useful diagnostically where a reliable MOG-Ab test is unavailable or gives a low positive and thus less specific result. Those with AQP4-Ab had single, predominantly central, long lesions as is typical of this disease (Tackley *et al.*, 2014a). Patients with multiple sclerosis had multiple small asymmetrical lesions, in keeping with the literature (Eden *et al.*, 2019).

Those with AQP4-Ab showed the greatest atrophy in the cervical and thoracic cord and grey matter as well as the most tissue damage as represented by the quantitative MRI metrics (fractional anisotropy, mean diffusivity and MTR). This damage was localized to areas of the cord involved during the acute attack. Those with persistent lesions had the worst metrics while areas of the cord that had never been involved were comparable to healthy volunteers. Lesions in AQP4-Ab disease therefore appeared to cause more localized damage than in multiple sclerosis and MOG-Ab disease. The involvement of the grey matter is expected in AQP4-Ab disease as it typically involves the central cord (Tackley *et al.*, 2014b).

In those with multiple sclerosis the overall mean metrics were abnormal when compared to healthy volunteers in grey matter volume, mean diffusivity, fractional anisotropy and MTR. However, there were no clear differences between those with lesions and those without. This suggests abnormalities in the normal-appearing spinal cord. This is an expected finding due to the background neurodegeneration and the findings of quantitative abnormalities in normal-appearing brain tissue in multiple sclerosis (Moll *et al.*, 2011). However, it must be taken into consideration that in multiple sclerosis because subclinical lesion activity is typical, and frequent enough MRI scans cannot be performed, normal-appearing tissue on MRI could include previous 'MRI resolved' lesions. Although in multiple sclerosis, lesions are not typically central, grey matter damage is well described in pathology (Geurts and Barkhof, 2008) and brain grey matter volume loss is predominant even in the early stages of multiple sclerosis (Calabrese *et al.*, 2007).

In MOG-Ab patients all reported metrics were normal except that of the grey matter volume in those with previous lesions. The findings in the MOG-Ab group are consistent with the clinical recovery in MOG-Ab patients, where in our

clinical practice we also see normalization of sensory and visual evoked potentials. This is not expected in multiple sclerosis or AQP4-Ab disease.

As mentioned, central cord involvement is well reported in those with AQP4-Ab and in MOG-Ab disease (Mariano *et al.*, 2019) and a recent study (Dubey *et al.*, 2019) described the 'H' sign seen on acute axial T₂ imaging where involvement of the cord appears to be limited to the grey matter. Grey matter involvement in MOG-Ab disease is proving to be increasingly important with a cortical phenotype now recognized (Ogawa *et al.*, 2017), documented grey matter involvement in ADEM-like disease (Hacohen *et al.*, 2017) and reports of acute flaccid myelitis associated with MOG-Ab (Dubey *et al.*, 2018; Wang *et al.*, 2018). Our finding of a reduction in grey matter volume in the MOG-Ab affected cord area further supports this and is the first quantitative evidence of long-term damage of grey matter. As measures such as fractional anisotropy and MTR are thought to better represent myelination and axonal integrity, (Miller *et al.*, 1998), the fact that they are unaffected may represent either that white matter is less affected or recovers better in the course of MOG-Ab disease but this grey matter involvement also requires further research into the underlying pathogenesis of MOG-Ab disease and the location of MOG expression within the CNS. The degree of grey matter atrophy in the cervical cord did not correlate with any clinical outcomes. However, as the predominant area involved in MOG-Ab disease is the thoracic cord and the most common symptoms that persist after an attack of myelitis are related to sphincter dysfunction, it may be the cervical cord does not capture this. We recently described the outcomes in myelitis in MOG-Ab disease (Mariano *et al.*, 2019) and found an association with conus lesions and long-term catheter requirements. However, conus involvement does not fully explain sphincter dysfunction in all patients with MOG-Ab. Given the importance of the grey matter in micturition pathways and sphincter control mechanisms (Fowler *et al.*, 2008), we hypothesize that this may be due to grey matter involvement in the lower cord and that improvements in thoracic cord imaging techniques would assist in studying this. Additionally, although our limited thoracic cord measurements did not correlate with disability outcomes, it must be noted that they only patient who reached EDSS 8 in the MOG-Ab cohort had the smallest thoracic cord volume and so the variability in the CSA values in the thoracic cord in MOG-Ab may suggest variable levels of tissue loss during the acute attack.

We then looked at the effect of relapses in the MOG-Ab disease group. It has been established that the presence of AQP4-Ab is predictive of relapsing disease and so it is recommended that all patients be treated with immunosuppressive treatment to prevent relapses (Weinshenker *et al.*, 2006; Jarius *et al.*, 2012). However, in MOG-Ab disease relapse rates of 34–46% (Jurynczyk *et al.*, 2017b; Cobo-Calvo *et al.*, 2018; Senanayake *et al.*, 2018) have been reported and so many patients may remain monophasic in their disease course and this has important treatment implications.

We compared those with relapsing disease and found that volumetric cord measures were lower in those with relapsing disease, even if the relapse occurred outside of the cord. It has been argued that if followed-up for long enough, all patients with MOG-Ab disease may eventually have a relapse and it is a continuum. However, our findings suggest that relapsing MOG-Ab disease may be distinct from monophasic disease.

We then considered the clinical relevance of the MRI metrics with regard to our three outcomes: disability, pain and fatigue. Our findings suggested that mean cervical cord area associates with disability independent of the disease type. It has already been suggested as an outcome measure for clinical trials in primary progressive multiple sclerosis (Cawley *et al.*, 2018) and has also been shown to be clinically useful in HTLV-1-associated neurological disease (Azodi *et al.*, 2017). Our hypothesis was that this measure would show an association with disability in our total cohort, independent of disease type. It was the only imaging metric that correlated with disability in a univariate analysis in each disease and, when combining diseases, it was the metric that built the strongest model using a stepwise regression. However, only 20% of disability is accounted for by this model and this is in keeping with other studies that have assessed cervical cord atrophy as measures of disability in multiple sclerosis (Tsagkas *et al.*, 2018; Song *et al.*, 2020). Correlations of disability with imaging outcomes is complex because disability scoring is imperfect and usually non-linear and imaging markers need to capture total pathology (volume loss and damage in remaining tissue) and account for the eloquence of different areas affected (although spinal cord is likely to be eloquent). Studies have largely only considered brain imaging markers as spinal cord imaging is notoriously difficult, particularly to standardize across centres to allow for larger cohorts. Future work may identify feasible methods for validating and incorporating these spinal cord measures into AQP4-Ab and MOG-Ab clinical trials together with brain imaging markers. Having an episode of myelitis in the context of NMOSD with AQP4-Abs is an independent predictor of pain separate to EDSS. Additionally, independent of disease type, we have shown for the first time, fractional anisotropy scores in the spinothalamic tracts associate with pain scores. We show that tract-specific analysis may be a useful tool when studying spinal cord involvement.

No spinal cord metric used in this study was able to capture sphincter dysfunction, particularly prominent in those with MOG-Ab. However, as described above, we feel that the thoracic cord would be more useful in the study of sphincter dysfunction as lower cord involvement is more common in MOG-Ab disease.

The final outcome that we studied was fatigue. There was no measure within the spinal cord that was able to explain fatigue and it is possible that fatigue is mainly driven by brain pathology although this may depend on the type of fatigue. It is a symptom that was experienced in all three conditions. Fatigue is a complex symptom with pathways that are still unclear (Braley and Chervin, 2010). It may be that

studies of functionality, such as resting state functional MRI, are more useful in better understanding this symptom. There is some evidence of its use in the brain (Jaeger *et al.*, 2019) but functional MRI of the spinal cord is an emerging field that may be useful in better understanding the complexity of such symptoms (Powers *et al.*, 2018).

Finally, we considered whether or not these metrics are able to discriminate these conditions. Our models showed a moderate ability to differentiate MOG-Ab disease cords from those with AQP4-Ab or multiple sclerosis, by using cord metrics alone, but the model for AQP4-Ab versus multiple sclerosis was not significant. In the brain it has been shown that clinical features of acute brain scans were able to differentiate the antibody-mediated conditions from multiple sclerosis (Jurynczyk *et al.*, 2017a). If we consider the acute spinal cord MRI features of AQP4-Ab and MOG-Ab myelitis, we have shown in a previous study that while there are notable differences i.e. predominance of the conus and multiple lesions in MOG-Ab, that 76% of patients with MOG-Ab and 89% of patients with AQP4-Ab had a long central lesion on their acute scan and so there is overlap in the acute setting between the antibody conditions. However, when we consider the features at follow-up, as we have shown in this study, the MOG-Ab group becomes distinct due to the significant recovery of both clinical MRI features and of the quantitative measures used in our study. While the predictive strength may not be adequate for individual patient diagnostic precision, these findings further support the evidence that MOG-Ab disease appears to be different from both AQP4-Ab disease and multiple sclerosis, which may be related to its milder phenotype with good recovery. In this cross-sectional comparison, AQP4-Ab and multiple sclerosis could not be accurately differentiated. Therefore, a prospective longitudinal study would be necessary to explore these conditions as one would expect worsening of all metrics in multiple sclerosis independent of relapse.

Limitations

We acknowledge the limitations of this study being sample size, where subtle differences may not be evident, and differences between the recognized disease characteristics within the groups that cannot be totally matched e.g. predominance of female sex, higher mean number of myelitis attacks and greater disability in AQP4-Ab disease and predominance of cervical cord involvement in multiple sclerosis as compared to the lower cord in antibody-mediated conditions. However, our groups were fairly well matched across many characteristics and we adjusted for those that were not in our analyses. Additionally, the homogeneity of a single-centre study where imaging is done on the same scanner (especially because obtaining reliable quantitative spinal cord imaging is challenging), and where consistency and accuracy of diagnosis is maximized (using the same highly specific assays and clinicians) is an advantage. The findings can then be used to build hypotheses and decide which protocols need to be aligned when taking observations forward into

multi-centre studies. Finally, technical limitations prevented the use of the quantitative MRI sequences in the thoracic cord.

Future perspectives

A longitudinal study would be important to see if the groups can be differentiated by the presence or absence of silent disease pathology and by combining brain, spinal cord and optical coherence tomography findings to capture the full spectrum of CNS involvement.

Conclusion

In this study we show that multimodal MRI provides us with valuable information about the spinal cord involvement in three different inflammatory demyelinating conditions. The conclusions of this study are based on the results of between-group and within-group comparisons that show consistent patterns, regardless of imaging metric, making the overall findings more compelling. This establishes a more robust understanding of these disorders. Myelitis with AQP4-Abs shows the most severe, localized damage in areas involved during the acute episode. In multiple sclerosis, metrics show significant change in comparison to healthy volunteers; however, the relationship with lesion location is not as pronounced. Finally, in MOG-Ab disease, metrics are comparable with healthy volunteers in all measures except that there is significant localized grey matter atrophy in affected areas of the cord. MOG-Ab disease is also moderately discriminated from AQP4-Ab disease and multiple sclerosis based on these quantitative metrics due to good recovery. Finally, we show that these metrics have clinical significance in their generic association with disability and pain scores.

Acknowledgements

We gratefully acknowledge all those who participated in this study. We thank Ms. Ana Cavey for her assistance with participant recruitment. We thank Mr. Michael Sanders, Mr. Jon Campbell, Mr. David Parker and all the staff at the Wellcome Centre for Integrative Neuroimaging. We thank Dr Maciej Jurynczyk for his insight on the use of discriminatory analysis.

Funding

We thank the Highly Specialised Commissioning Team for funding the Neuromyelitis Optica service in Oxford. R.M. is undertaking graduate studies funded by scholarships from the Rhodes Trust and the Oppenheimer Memorial Trust. MRI scans were funded by a Research and Development Fund belonging to the principal investigator, J.A.P. Y.K. was supported by the National Natural Science Foundation of China (No. 81871436) and the Informatization Special

Project of Chinese Academy of Sciences (No. XXH13506–306).

Competing interests

The authors report no competing interests.

Supplementary material

Supplementary material is available at *Brain* online.

References

- Altmann D, Button T, Schmierer K, Hunter K, Tozer D, Wheeler-Kingshott C, et al. Sample sizes for lesion magnetisation transfer ratio outcomes in remyelination trials for multiple sclerosis. *Mult Scler Relat Disord* 2014; 3: 237–43.
- Andersson JLR, Skare S, Ashburner J. How to correct susceptibility distortions in spin-echo echo-planar images: application to diffusion tensor imaging. *Neuroimage* 2003; 20: 870–88.
- Andersson JLR, Sotiropoulos SN. An integrated approach to correction for off-resonance effects and subject movement in diffusion MR imaging. *Neuroimage* 2016; 125: 1063–78.
- Azodi S, Nair G, Enose-Akahata Y, Charlip E, Vellucci A, Cortese I, et al. Imaging spinal cord atrophy in progressive myelopathies: HTLV-I-associated neurological disease (HAM/TSP) and multiple sclerosis. *Ann Neurol* 2017; 82: 719–28.
- Benedetti B, Valsasina P, Judica E, Martinelli V, Ghezzi A, Capra R, et al. Grading cervical cord damage in neuromyelitis optica and MS by diffusion tensor MRI. *Neurology* 2006; 67: 161.
- Braley TJ, Chervin RD. Fatigue in multiple sclerosis: mechanisms, evaluation, and treatment. *Sleep* 2010; 33: 1061.
- Calabrese M, Atzori M, Bernardi V, Morra A, Romualdi C, Rinaldi L, et al. Cortical atrophy is relevant in multiple sclerosis at clinical onset. *J Neurol* 2007; 254: 1212–20.
- Casserly C, Seyman EE, Alcaide-Leon P, Guenette M, Lyons C, Sankar S, et al. Spinal cord atrophy in multiple sclerosis: a systematic review and meta-analysis. *J Neuroimaging* 2018; 28: 556–586.
- Cawley N, Tur C, Prados F, Plantone D, Kearney H, Abdel-Aziz K, et al. Spinal cord atrophy as a primary outcome measure in phase II trials of progressive multiple sclerosis. *Mult Scler J* 2018; 24: 932–41.
- Chien C, Scheel M, Schmitz-Hübsch T, Borisow N, Ruprecht K, Bellmann-Strobl J, et al. Spinal cord lesions and atrophy in NMOSD with AQP4-IgG and MOG-IgG associated autoimmunity. *Mult Scler J* 2019; 25: 1926–36.
- Ciccharelli O, Cohen JA, Reingold SC, Weinschenker BG, Amato MP, Banwell B, et al. Spinal cord involvement in multiple sclerosis and neuromyelitis optica spectrum disorders. *Lancet Neurol* 2019; 18: 185–97.
- Cobo-Calvo A, Ruiz A, Maillart E, Audoin B, Zephir H, Bourre B, et al. Clinical spectrum and prognostic value of CNS MOG autoimmunity in adults. *Neurology* 2018; 90: e1858–e1869.
- Dubey D, Pittock SJ, Krecke KN, Morris PP, Sechi E, Zaleski NL, et al. Clinical, radiologic, and prognostic features of myelitis associated with myelin oligodendrocyte glycoprotein autoantibody. *JAMA Neurol* 2018; 55905: 1–9.
- Dubey D, Pittock SJ, Krecke KN, Morris PP, Sechi E, Zaleski NL, et al. Clinical, radiologic, and prognostic features of myelitis associated with myelin oligodendrocyte glycoprotein autoantibody. *JAMA Neurol* 2019; 76: 301–9.

- Eden D, Gros C, Badji A, Dupont SM, De Leener B, Maranzano J, et al. Spatial distribution of multiple sclerosis lesions in the cervical spinal cord. *Brain* 2019; 142: 633–46.
- Faul F, Erdfelder E, Lang A-G, Buchner A. GPower 3: a flexible statistical power analysis program for the social, behavioral, and biomedical sciences. *Behav Res Methods* 2007; 39: 175.
- Filippi M, Preziosa P, Banwell BL, Barkhof F, Ciccarelli O, De Stefano N, et al. Assessment of lesions on magnetic resonance imaging in multiple sclerosis: practical guidelines. *Brain* 2019; 142: 1858–75.
- Flanagan EP, Weinshenker BG, Krecke KN, Lennon VA, Lucchinetti CF, McKeon A, et al. Short myelitis lesions in aquaporin-4-IgG-positive neuromyelitis optica spectrum disorders. *JAMA Neurol* 2015a; 72: 81–7.
- Flanagan EP, Weinshenker BG, Krecke KN, Pittock SJ. Asymptomatic myelitis in neuromyelitis optica and autoimmune aquaporin-4 channelopathy. *Neurol Clin Pract* 2015b; 5: 175–7.
- Fowler C, Griffiths D, De Groat W. The neural control of micturition. *Nat Rev Neurosci* 2008; 9: 453.
- Geurts JJ, Barkhof F. Grey matter pathology in multiple sclerosis. *Lancet Neurol* 2008; 7: 841–51.
- Hacohen Y, Mankad K, Chong WK, Barkhof F, Vincent A, Lim M, et al. Diagnostic algorithm for relapsing demyelinating syndromes of the CNS in children including myelin oligodendrocyte glycoprotein. *Lancet* 2017; 389: S41.
- Jaeger S, Paul F, Scheel M, Brandt A, Heine J, Pach D, et al. Multiple sclerosis-related fatigue: altered resting-state functional connectivity of the ventral striatum and dorsolateral prefrontal cortex. *Mult Scler J* 2019; 25: 554–64.
- Jarius S, Ruprecht K, Wildemann B, Kuempfel T, Ringelstein M, Geis C, et al. Contrasting disease patterns in seropositive and seronegative neuromyelitis optica: a multicentre study of 175 patients. *J Neuroinflammation* 2012; 9: 14.
- Jenkinson M, Beckmann CF, Behrens TE, Woolrich MW, Smith SM. *FSL. Neuroimage* 2012; 62: 782–90.
- Jurynczyk M, Galdes R, Probert F, Woodhall MR, Waters P, Tackley G, et al. Distinct brain imaging characteristics of autoantibody-mediated CNS conditions and multiple sclerosis. *Brain* 2017a; 140: 617–27.
- Jurynczyk M, Messina S, Woodhall MR, Raza N, Everett R, Rocafernandez A, et al. Clinical presentation and prognosis in MOG-antibody disease: a UK study. *Brain* 2017b; 140: 3128–38.
- Kitley J, Leite MI, Nakashima I, Waters P, McNeill B, Brown R, et al. Prognostic factors and disease course in aquaporin-4 antibody-positive patients with neuromyelitis optica spectrum disorder from the United Kingdom and Japan. *Brain* 2012; 135: 1834–49.
- Kitley J, Waters P, Woodhall M, Leite MI, Murchison A, George J, et al. Neuromyelitis optica spectrum disorders with aquaporin-4 and myelin-oligodendrocyte glycoprotein antibodies a comparative study. *JAMA Neurol* 2014; 71: 276–83.
- Klawiter EC, Xu J, Naismith RT, Benzinger TL, Shimony JS, Lancia S, et al. Increased radial diffusivity in spinal cord lesions in neuromyelitis optica compared with multiple sclerosis. *Mult Scler J* 2012; 18: 1259–68.
- Kleiter I, Gahlen A, Borisow N, Fischer K, Wernecke KD, Wegner B, et al. Neuromyelitis optica: evaluation of 871 attacks and 1,153 treatment courses. *Ann Neurol* 2016; 79: 206–16.
- De Leener B, Lévy S, Dupont SM, Fonov VS, Stikov N, Louis Collins D, et al. SCT: spinal Cord Toolbox, an open-source software for processing spinal cord MRI data. *Neuroimage* 2017; 145: 24–43.
- Liu Y, Wang J, Daams M, Weiler F, Hahn HK, Duan Y, et al. Differential patterns of spinal cord and brain atrophy in NMO and MS. *Neurology* 2015; 84: 1465 LP– 72.
- Lucchinetti CF, Guo Y, Popescu BFG, Fujihara K, Itoyama Y, Misu T. The pathology of an autoimmune astrocytopathy: lessons learned from neuromyelitis optica. *Brain Pathol* 2014; 24: 83–97.
- Mariano R, Messina S, Kumar K, Kuker W, Leite MI, Palace J. Comparison of clinical outcomes of transverse myelitis among adults with myelin oligodendrocyte glycoprotein antibody vs aquaporin-4 antibody disease. *JAMA Netw Open* 2019; 2: e1912732.
- Matthews L, Kolind S, Brazier A, Leite MI, Brooks J, Traboulsée A, et al. Imaging surrogates of disease activity in neuromyelitis optica allow distinction from multiple sclerosis. *PLoS One* 2015; 10: 1–19.
- McCarthy P. FSLeys. 2019. https://doi.org/10.5281/zenodo.3403671#.XbAuog_Uj0t (23 October 2019, date last accessed).
- Miller DH, Grossman RI, Reingold SC, McFarland HF. The role of magnetic resonance techniques in understanding and managing multiple sclerosis. *Brain* 1998; 121: 3–24.
- Moccia M, Ruggieri S, Ianniello A, Toosy A, Pozzilli C, Ciccarelli O. Advances in spinal cord imaging in multiple sclerosis. *Ther Adv Neurol Disord* 2019; 12: 1756286419840593.
- Moll NM, Rietsch AM, Thomas S, Ransohoff AJ, Lee JC, Fox R, et al. Multiple sclerosis normal-appearing white matter: pathology-imaging correlations. *Ann Neurol* 2011; 70: 764–73.
- Naismith RT, Xu J, Klawiter EC, Lancia S, Tutlam NT, Wagner JM, et al. Spinal cord tract diffusion tensor imaging reveals disability substrate in demyelinating disease. *Neurology* 2013; 80: 2201.
- Ogawa R, Nakashima I, Takahashi T, Kaneko K, Akaishi T, Takai Y, et al. MOG antibody-positive, benign, unilateral, cerebral cortical encephalitis with epilepsy. *Neurol Neuroimmunol Neuroinflamm* 2017; 4:
- Olsson T, Barcellos LF, Alfredsson L. Interactions between genetic, lifestyle and environmental risk factors for multiple sclerosis. *Nat Rev Neurol* 2016; 13: 26–36.
- Pandit L, Asgari N, Apiwatanakul M, Palace J, Paul F, Leite M, et al. Demographic and clinical features of neuromyelitis optica: a review. *Mult Scler J* 2015; 21: 845–53.
- Pessôa FMC, Lopes FCR, Costa JVA, Leon SVA, Domingues RC, Gasparetto EL. The cervical spinal cord in neuromyelitis optica patients: a comparative study with multiple sclerosis using diffusion tensor imaging. *Eur J Radiol* 2012; 81: 2697–701.
- Powers JM, Ioachim G, Stroman PW. Ten key insights into the use of spinal cord fMRI. *Brain Sci* 2018; 8: 173.
- Prados F, Barkhof F. Spinal cord atrophy rates: ready for prime time in multiple sclerosis clinical trials? *Neurology* 2018; 91: 157–8.
- Reich DS, White R, Cortese IC, Vuolo L, Shea CD, Collins TL, et al. Sample-size calculations for short-term proof-of-concept studies of tissue protection and repair in multiple sclerosis lesions via conventional clinical imaging. *Mult Scler J* 2015; 21: 1693–704.
- Senanayake B, Jitrapaikulsan J, Aravinthan M, Wijesekera JC, Ranawaka UK, Riffisy MT, et al. Seroprevalence and clinical phenotype of MOG-IgG-associated disorders in Sri Lanka. *J Neurol Neurosurg Psychiatry* 2018; 90: 1381.
- Smith SM, Jenkinson M, Woolrich MW, Beckmann CF, Behrens TE, Johansen-Berg H, et al. Advances in functional and structural MR image analysis and implementation as FSL. *Neuroimage* 2004; 23: S208–19.
- Song X, Li D, Qiu Z, Su S, Wu Y, Wang J, et al. Correlation between EDSS scores and cervical spinal cord atrophy at 3T MRI in multiple sclerosis: a systematic review and meta-analysis. *Mult Scler Relat Disord* 2020; 37: 101426.
- Stroman PW, Bacon M, Schwab JM, Bosma R, Cadotte D, Carlstedt T, et al. The current state-of-the-art of spinal cord imaging: methods. *Neuroimage* 2015a; 84: 1070–81.
- Stroman PW, Schwab JM, Bacon M, Bosma R, Cadotte DW, Carlstedt T, et al. The current state-of-the-art of spinal cord imaging: applications. *Neuroimage* 2015b; 1082–93.
- Tackley G, Kuker W, Palace J. Magnetic resonance imaging in neuromyelitis optica. *Mult Scler* 2014; 1153–64.
- Tan CT, Mao Z, Wingerchuk DM, Qiu W, Hu X, Weinshenker BG. International consensus diagnostic criteria for neuromyelitis optica spectrum disorders. *Neurology* 2016; 86: 491–2.
- Tsagkas C, Magon S, Gaetano L, Pezold S, Naegelin Y, Amann M, et al. Spinal cord volume loss. *Neurology* 2018; 91: e349–358.

- Wang C, Narayan R, Greenberg B. Anti-myelin oligodendrocyte glycoprotein antibody associated with gray matter predominant transverse myelitis mimicking acute flaccid myelitis: a presentation of two cases. *Pediatr Neurol* 2018; 86: 42–5.
- Waterman CL, Currie RA, Cottrell LA, Dow J, Wright J, Waterfield CJ, et al. An integrated functional genomic study of acute phenobarbital exposure in the rat. *BMC Genomics* 2010; 11: 9.
- Waters P, Woodhall M, O'Connor KC, Reindl M, Lang B, Sato DK, et al. MOG cell-based assay detects non-MS patients with inflammatory neurologic disease. *Neurol Neuroimmunol Neuroinflamm* 2015; 2: e89.
- Weinshenker BG, Wingerchuk DM, Vukusic S, Linbo L, Pittock SJ, Lucchinetti CF, et al. Neuromyelitis optica IgG predicts relapse after longitudinally extensive transverse myelitis. *Ann Neurol* 2006; 59: 566–569.
- Wingerchuk DM, Pittock SJ, Waters PJ, Weinshenker BG, Bennett JL, Jarius S. Evaluation of aquaporin-4 antibody assays. *Clin Exp Neuroimmunol* 2014; 5: 290–303.